JACS
JOURNAL OF THE AMERICAN CHEMICAL SOCIETY
Article
pubs.acs.org/JACS

Input-Dependent Induction of Oligonucleotide Structural Motifs for Performing Molecular Logic

Tao Li, Damian Ackermann, Anna M. Hall, and Michael Famulok*

Life and Medical Science (LIMES) Institute, Program Unit Chemical Biology and Medicinal Chemistry, University of Bonn, Gerhard-Domagk-Str. 1, 53121 Bonn, Germany

Supporting Information

ABSTRACT: The K^+–H^+-triggered structural conversion of multiple nucleic acid helices involving duplexes, triplexes, G-quadruplexes, and i-motifs is studied by gel electrophoresis, circular dichroism, and thermal denaturation. We employ the structural interconversions for perfoming molecular logic operations, as verified by fluorimetry and colorimetry. Short G-rich and C-rich cDNA and RNA single strands are hybridized to produce four A-form and B-form duplexes. Addition of K^+ triggers the unwinding of the duplexes by inducing the folding of G-rich strands into DNA- or RNA G-quadruplex mono- and multimers, respectively. We found a decrease in pH to have different consequences on the resulting structural output, depending on whether the C-rich strand is DNA or RNA: while the protonated C-rich DNA strand folds into at least two isomers of a stable i-motif structure, the protonated C-rich RNA strand binds a DNA/RNA hybrid duplex to form a Y·RY parallel triplex. When using K^+ and H^+ as external stimuli, or inputs, and the induced G-quadruplexes as reporters, these structural interconversions of nucleic acid helices can be employed for performing logic-gate operations. The signaling mode for detecting these conversions relies on complex formation between DNA or RNA G-quadruplexes (G4) and the cofactor hemin. The G4/hemin complexes catalyze the H_2O_2-mediated oxidation of peroxidase substrates, resulting in a fluorescence or color change. Depending on the nature of the respective peroxidase substrate, distinct output signals can be generated, allowing one to operate multiple logic gates such as NOR, INH, or AND.

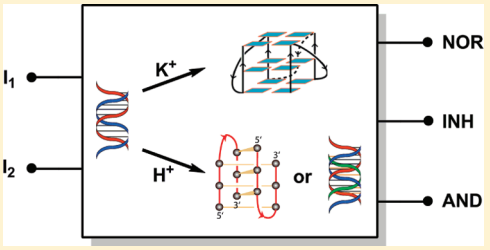

INTRODUCTION

Under standard conditions, two complementary strands of single-stranded (ss) DNA or RNA hybridize to form a Watson–Crick paired double-helix.[1] Two types of triple-stranded helices of nucleic acids, parallel (Y·RY) and antiparallel (R·RY), can form when a third strand binds to the major groove of a Watson–Crick duplex via Hoogsteen hydrogen bonding.[2,3] A Y·RY triplex is built on the C^+·GC and T·AT base triplets, of which the formation of C^+·GC is only allowed at acidic pH (below 6) when cytosine residues become protonated. Under acidic conditions, a protonated C-rich ssDNA strand can fold into a higher-order four-stranded structure called i-motif, consisting of two parallel duplexes whose C^+·C base pairs are fully intercalated.[4] RNA i-motif structures are also found under similar conditions, but these exhibit considerably lower stability than do the DNA counterparts.[5] An intramolecular i-motif can adopt more than one folding topology,[6] as evidenced by NMR and gel electrophoresis.[6,7] Another four-stranded helix, the G-quadruplex (G4), is formed by G-rich ssDNA or RNA in the presence of monovalent cations like Na^+ or K^+.[8] The G4-motif is built on the Hoogsteen hydrogen-bonded guanine tetrads that stack on one another, stabilized by van der Waals interactions.[9,10] Monovalent cations like K^+ can facilitate the π–π stacking of DNA and RNA G-quadruplex monomers to form stable dimers and trimers.[11−14]

There are some intrinsic relationships between these helical structures of nucleic acids. Two G-rich and C-rich strands can either hybridize to form a Watson–Crick double helix, or they individually fold into G-quadruplex and i-motif in the presence of K^+ and H^+. As a consequence, a potential competition can occur between duplex- and G-quadruplex or i-motif formation, which has been observed in biologically relevant nucleic acids like human telomeric DNA and others.[15,16] Similarly, at acidic pH, both the i-motif and a C^+·GC triplex can form.[17] Hence, an additional level of competition, between i-motif- and triplex-formation, and between G-quadruplex and C^+·GC triplex formation, may occur under certain conditions in response to external stimuli like K^+ and H^+. When equipped with appropriate fluorescent or other indicators, the response of nucleic acids to external stimuli can directly be followed. This read-out can be transduced into a Boolean logic operation, in which the presence or absence of a stimulus and the increase or decrease of the readout signal are related to a 1/0 event. Along this route, numerous molecular logic gates have been realized by employing various nucleic acids and read-out formats.[18−20] However, a nucleic acid reconfiguration system covering the complexity of the possible interconversions of nucleic acids from homo- and heteroduplexes to triplexes, G-quadruplexes, and i-motifs has not yet been systematically devised.[21]

Received: November 19, 2011
Published: January 31, 2012

dx.doi.org/10.1021/ja2108883 | J. Am. Chem. Soc. 2012, 134, 3508–3516

Herein, we describe such a system consisting of G-rich and C-rich short oligonucleotides (DNA and RNA), in which K^+ and/or H^+ are systematically employed as distinct external triggers that induce the respective structural conversion. We have used polyacrylamide gel electrophoresis (PAGE) and circular dichroism (CD) to analyze the variety of interconversions between duplex/triplex, duplex/G-quadruplex, duplex/i-motif, and triplex/G-quadruplex that occur in response to the external trigger. We then employ the respective structural conversions of nucleic acid helices for operating a versatile molecular logic system with K^+ and H^+ as two inputs. As the reporter system for each signal output, we use the hemin−G-quadruplex complex in the presence of peroxidase substrates. This detection relies on the specific binding of the catalytic cofactor hemin by DNA and RNA G-quadruplexes that mimics horseradish peroxidase (HRP) and catalyzes the H_2O_2-mediated oxidation of peroxidase substrates.[22,23] To achieve multiple logic gate operations (NOR, INH, AND, etc.), distinct output signals are generated by using peroxidase substrates that function under the different conditions applied for each operation.

EXPERIMENTAL SECTION

Oligonucleotides and Structural Conversion. HPLC-purified and MS-verified oligonucleotides were obtained from METABION (Martinsried, Germany). The oligonucleotides were prepared in pH 7.4 TE buffer (10 mM Tris-HCl, 1 mM EDTA), and their concentrations were quantified by using a TECAN Infinite M200 multimode microplate reader (Tecan Austria GmbH) with a NanoQuant plate. Two complementary strands were mixed in a 1:1 molar ratio, heated at 87 °C for 10 min, and then slowly cooled to room temperature, allowing two complementary strands to be hybridized and form a Watson−Crick double helix. Next, the duplexes were diluted to required concentrations with 50 mM Tris-Ac buffer (pH 8.5). After addition of 20 mM K^+ and H^+ (pH 8.5→4.5), each duplex was incubated at 37 °C and slightly shaken for 5 h, allowing the unwinding of duplexes and formation of other helical structures such as G-quadruplex, i-motif, and triplex.

Native PAGE. Nondenaturing polyacrylamide gel (18%) was prepared in 50 mM, pH 8.5/4.5 Tris-Ac buffer with/without 20 mM KCl. In each case, the same buffer was used for gel electrophoresis. Before loading samples, 20 μL of 10 μM oligonucleotides was mixed with 4 μL of 6× loading buffer (30% glycerol, 0.05% xylene cyanol FF) and cooled to 4 °C. Gel electrophoresis was run at 4 °C for 16 h under a voltage of 4 V/cm at pH 8.5 and 5 V/cm at pH 4.5. The gels were then immersed in 25% isopropanol for 15 min, then stained in the Stains-All solution (0.01% Stains-All, 15 mM Tris-Ac (pH 8.5), 25% isopropanol) at dark for 4 h, followed by destaining in water under moderate light until the gels turned clear, and finally photographed with a personal camera.

CD Measurements. A JASCO J-810 spectropolarimeter (Tokyo, Japan) was utilized to collect the CD spectra of 20 μM oligonucleotides (each strand concentration) at room temperature at four input modes. The optical chamber (1 mm optical path length) was deoxygenated with dry purified nitrogen before use and kept in the nitrogen atmosphere during experiments. Three scans from 200 to 320 nm were accumulated and averaged. In each case, the background of the buffer solution was subtracted from the CD data.

Melting Curves. The melting curves of oligonucleotides (each strand concentration is 2.5 μM) in 50 mM Tris-Ac buffer (pH 8.5/4.5, with/without 20 mM KCl) were recorded by a UV spectrometer equipped with a temperature-controlled water bath, with a rate of 0.5 °C/min. Data were collected every 0.1 °C. When duplexes and triplexes were melted, the absorbance was always monitored at 260 nm, whereas the absorbance at 295 nm was monitored for melting G-quadruplexes and i-motif. The melting curves were plotted using normalized absorbance versus temperature, and then differentiated to give the melting temperatures (T_m) of nucleic acid helices.

Logic Operations. After the structural conversion of nucleic acid helices at four input modes, hemin was added and incubated at room temperature for over 1 h, allowing hemin to combine with G-quadruplex to form the hemin−G-quadruplex catalytic complex. Next, different peroxidase substrates were added, followed by H_2O_2 to initiate the enzymatic reaction. Finally, the fluorescence and absorption spectra of different reaction mixtures were recorded by a Thermo Scientific Varioskan Flash spectral scanning multimode reader (Vantaa, Finland).

RESULTS AND DISCUSSION

K^+−H^+-Triggered Reconfiguration of Nucleic Acid Structures. Depending on the applied conditions, the G/C-rich oligonucleotides can potentially rearrange into a variety of structural motifs. These range from A- and B-type homo- and heteroduplexes, a C^+·GC triple helix, G-quadruplexes, and i-motif structures. Under certain conditions, these oligonucleotides engange in various structural motifs that have the potential to interconvert from one to another. To establish conditions for interconversion and to analyze the various motifs formed, we designed short G-rich and C-rich cDNA- and RNA-oligonucleotides D1, D2, R1, and R2 that easily hybridize to produce four Watson−Crick duplexes. Upon addition of K^+ and H^+, different structural conversions are expected to occur to these duplexes (Figure 1a), due to the difference in the stability of various structural motifs.

We employed PAGE under nondenaturing conditions to analyze the structures formed by the different pairs of oligonucleotides under different conditions (Figure 2, lanes 1−4), with four constituent strands as the controls (lanes 5−8). At pH 8.5 and in the absence of K^+-ions, only a single band appears for each duplex (Figure 2a, lanes 1−4), indicating that each pair of complementary strands forms a stable double helical structure. The corresponding CD spectra show that the DNA duplex (D1D2) has a positive peak near 270 nm and another smaller one around 220 nm (Figure 3a), consistent with the CD characteristics of a B-form conformation.[24] The RNA duplex (R1R2) has a negative peak at 213 nm and a positive one near 270 nm with a shoulder around 250 nm, indicating that this duplex adopts a A-form conformation.[24] The CD characteristics of R1D2 are more similar to those of A-form RNA than to those of B-form DNA, indicating that the global conformation of this DNA/RNA hybrid duplex is A-form. However, the CD spectrum of D1R2 shows it appears to adopt an intermediate conformation, neither B-form nor A-form. A similar phenomenon also occurred to other DNA/RNA hybrid duplexes.[25] The RNA and DNA/RNA hybrid duplexes all have a lower mobility than the DNA duplex (Figure 2a), consistent with previous observations.[26−28] Under the same conditions at pH 8.5 and in the absence of K^+-ions, the C-rich control strands R2 and D2 have typical CD characteristics of poly-C single strands,[29,30] with a positive band near 275 nm (Figure 3a). The two G-rich strands, especially R1, have CD features of parallel G-quadruplexes, with a positive band near 260 nm and negative one around 240 nm.[24] This suggests that D1 and R1 fold into parallel G-quadruplexes even in the absence of K^+. The folded R1 runs slowly in PAGE (Figure 2a, lane 7), while D1 is smeared (lane 5), presumably due to the poor thermal stability of its G-quadruplex structure (no obvious T_m, see Figure S1 in the Supporting Information) in the absence of metal cations. The intact but widened band of folded D1 without K^+ is only observed at acidic pH (Figure 2c,

dx.doi.org/10.1021/ja2108883 | J. Am. Chem. Soc. 2012, 134, 3508−3516

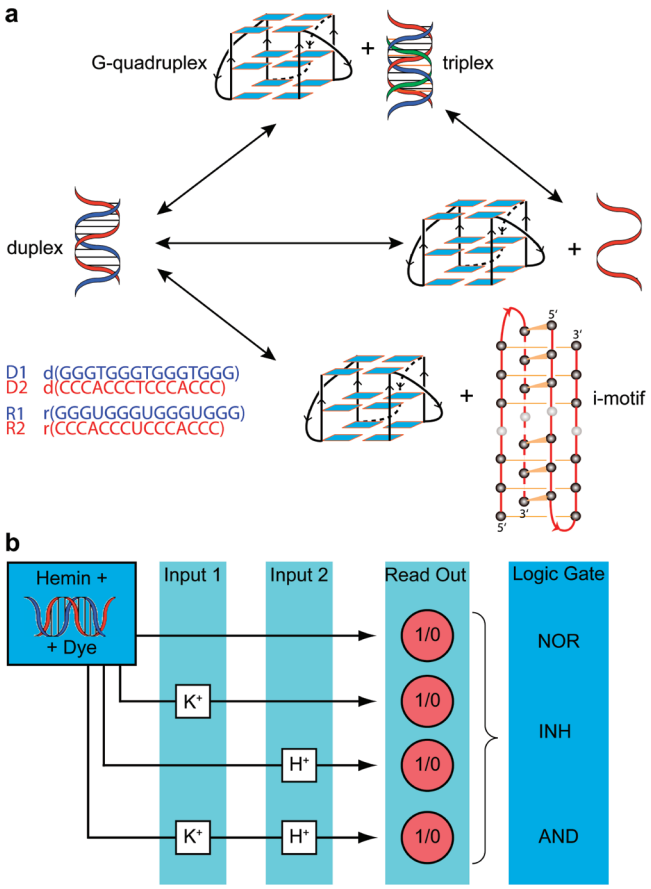

Figure 1. Oligonucleotide strand interconversions and construction of the logic gates. (a) Schematic for the interconversion of nucleic acid helical structures triggered by K^+ and H^+, two G-rich (blue), and two C-rich (red) oligonucleotides used here. In the G-quadruplex scheme, the blue rectangles represent G-residues, and the black lines the sugar–phosphate backbone. In the i-motif scheme, the dark gray and light gray spheres represent C and A residues, respectively, the red lines the sugar–phosphate backbone, and the orange lines the connection between each residue by H-bonds. The loop residues in the G-quadruplex and i-motif structure are not shown. (b) Multiple logic gate operations based on the structural conversion of nucleic acid helices, with K^+ and H^+ as two inputs.

lane 5), where the gel electrophoretic mobility is lower than at basic pH.

Upon incubation with K^+, some dramatic changes are observed in the electrophoretic behavior of the different oligonucleotides (Figure 2b). More than one band is clearly observed in lanes 1 and 4, with the same mobility as the corresponding constituent strands (lanes 5, 8 and 6, 7, respectively). Thus, the D1D2 and D1R2 duplexes are subject to unwinding induced by K^+. No unwinding of the RNA duplex R1R2 and the heteroduplex R1D2 occurs under these conditions (Figure 2b, lane 2).

The K^+-triggered structural changes are further confirmed by CD measurements (Figure 3b). In the CD spectra of D1D2 and D1R2, a positive band near 260 nm together with a negative one around 240 nm is observed, consistent with the formation of parallel G-quadruplexes. This implies a duplex-to-G-quadruplex conversion of D1D2 and D1R2. In contrast, the CD spectra of R1R2 and R1D2 still remain the typical characteristics of A-form duplexes, indicating the double-stranded helix is the dominant structure of R1R2 and R1D2 even in the presence of K^+. Interestingly, the folded D1 and R1 in K^+ solution display more than one band in the gel (Figure 2b, lanes 5 and 7), suggesting the presence of at least two distinct structures in these samples. Previous studies have clearly demonstrated that G-rich strands with three single-base loops only occur in one folding topology, an intramolecular parallel G-quadruplex.[31−33] This renders the existence of G-quadruplex isomers of D1 and R1 unlikely. The two or more bands presumably originate from the formation of G-quadruplex multimers like dimers and trimers formed by two or three stacked G-quadruplex monomers (Figure S2 in the Supporting Information). These superstructures of DNA and RNA G-quadruplexes, facilitated by monovalent cations, particularly K^+, have been observed previously by gel electrophoresis and mass spectrometry.[11−14] Under our conditions, a small amount of dimer of folded D1 is clearly observed together with a larger amount of G-quadruplex in its monomeric form. In contrast, equal amounts of mono- and dimeric R1-quadruplex are formed together with a smaller amount of trimeric R1-quadruplex, indicating that the RNA G-quadruplex appears to more easily form multimers than does the DNA counterpart.

Upon lowering the pH to 4.5 in the absence of K^+-ions, different phenomena are observed in PAGE (Figure 2c). In lanes 1 and 3, there is one band with the same mobility as D1 or R1, respectively, and a band with the same mobility as D2 (see lanes 5, 7, 8). This demonstrates that both duplexes D1D2 and R1D2 completely unwind at pH 4.5, presumably by forming i-motif structures. Formation of the i-motif is evidenced by CD spectroscopy (Figure 3c). Both D1D2 and R1D2 display a positive band near 290 nm in the corresponding CD spectra (Figure 3c, left panel). The CD spectrum of the D2 control has a dominant positive band near 290 nm and a negative one around 260 nm (Figure 3c, right panel), consistent with the characteristics of an i-motif structure.[24] In contrast, the CD characteristics of R2 still remain as those of an unfolded single strand, because the i-motif structure of C-rich RNA is so unstable that it only exists at millimolar strand concentrations and at low temperature.[5] Note that the T_m value of folded D2 is increased as the strand concentration increases (see Figure S3 in the Supporting Information), which is a typical characteristic of an intermolecular structure.[34] That is, D2 forms the intermolecular i-motif structure at acidic pH, which should be attributed to its three short loops (each composed of one T residue) not compatible with the intramolecular folding of i-motif.[7] In principle, an intramolecular i-motif has four possible folding configurations,[6] and two bands of i-motif isomers can be observed in gel electrophoresis.[7] Similarly, two bands of D2 are always observed in PAGE at acidic pH (Figure 2c and d, lanes 1, 3, 8). Considering only one phase transition in the melting profile of folded D2 (see Figure S1), the two bands of D2 suggest that this intermolecular i-motif also has more than one possible folding configuration, as described previously (see Figure S4 in the Supporting Information for the proposed structures of the intermolecular i-motif).[7] In case of D1R2, we observe two strong bands in purple under acidic conditions (Figure 2c, lane 4), and a faint band in cyan between them, presumably corresponding to D1 folded into G4 (red asterisk; compare with lane 5). This band indicates that a small amount of D1R2 unwinds, but neither of the other two bands (purple) corresponds to R2 (compare lane 6). On the other hand, the corresponding CD spectrum of D1R2 in Figure 3c (line in

dx.doi.org/10.1021/ja2108883 | J. Am. Chem. Soc. 2012, 134, 3508–3516

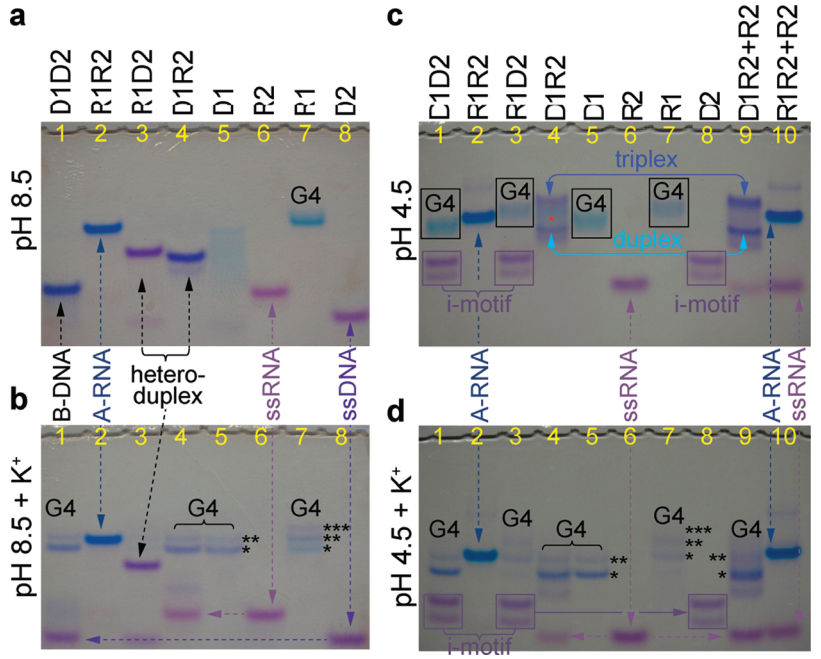

Figure 2. Electrophoretograms of 0.2 nmol of oligonucleotides in 18% native gels under different conditions: (a) 50 mM, pH 8.5 Tris-Ac buffer; (b) 50 mM, pH 8.5 Tris-Ac buffer with 20 mM KCl; (c) 50 mM, pH 4.5 Tris-Ac buffer; red asterisk, a very small amount of G4 can be detected; and (d) 50 mM, pH 4.5 Tris-Ac buffer with 20 mM KCl. In lanes 4 and 9, the bands labeled "heteroduplex" or "duplex", respectively, most likely correspond to residual D1R2 heteroduplex, but we do not have unambiguous proof that this is the case. *G4 monomer, **G4 dimer, ***G4 trimer. The framed bands labeled "i-motif" in (c) and (d) represent two i-motif isomers.

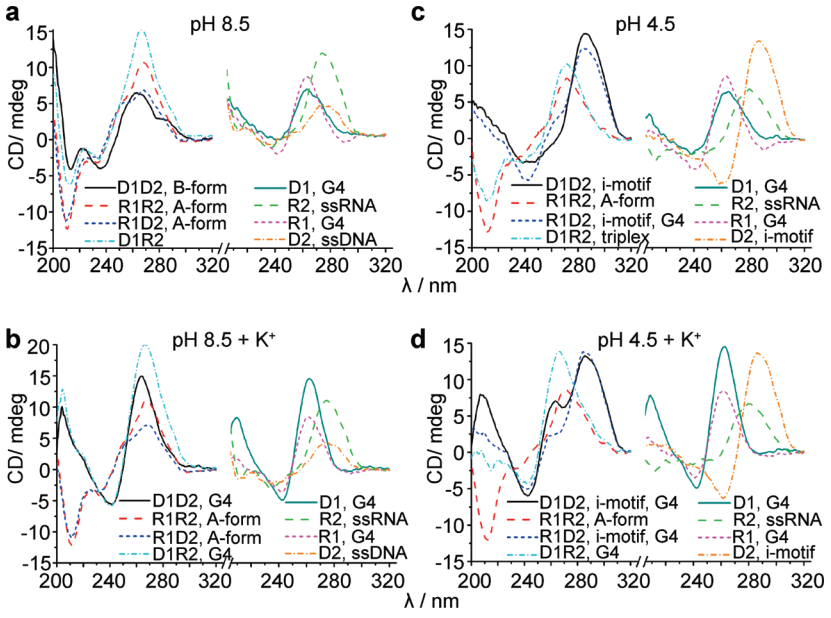

Figure 3. CD spectra of 20 μM oligonucleotides (each strand concentration) under different conditions: (a) 50 mM, pH 8.5 Tris-Ac buffer; (b) 50 mM, pH 8.5 Tris-Ac buffer with 20 mM KCl; (c) 50 mM, pH 4.5 Tris-Ac buffer; and (d) 50 mM, pH 4.5 Tris-Ac buffer with 20 mM KCl.

cyan) at pH 4.5 appears to be very similar to that of the A-form duplex D1R2 observed at pH 8.5 (Figure 3a, left panel, cyan line). However, the main difference between D1R2 at pH 8.5 vs 4.5 is revealed by their melting behavior: the T_m of D1R2 at pH 4.5 is increased by 7.8 °C as compared to the T_m measured at pH 8.5 (Figure 4). The ΔT_m of 7.8 °C suggests the formation of a triple helix structure R2$^+$·D1R2 that accommodates the protonated R2 strand. This notion is supported by the fact that the cytosine base is easily protonated under acidic conditions, allowing the formation of either an i-motif or a C$^+$·GC triplex.[3,35] Our CD measurements (Figure 3c, right panel, green line) indicate that the C-rich R2 oligonucleotide prefers to form the single strand structure rather than the RNA i-motif structure. The protonated, single-stranded R2 can readily bind to the major groove of the duplex D1R2 by forming C$^+$·GC base triplets, resulting in a Y·RY parallel triplex.[2,3] To investigate this hypothesis, we added an equivalent of R2 to the D1R2, and an equivalent of R2 to the R1R2 under the same conditions (Figure 2c, lanes 9 and 10). Analysis by PAGE revealed a significant increase of the band that corresponds to

dx.doi.org/10.1021/ja2108883 | J. Am. Chem. Soc. 2012, 134, 3508–3516

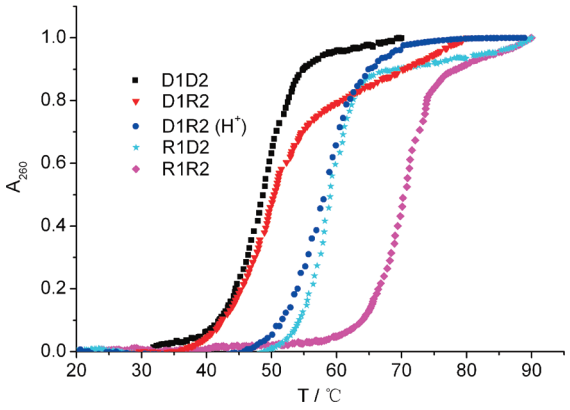

Figure 4. Melting profiles of 2.5 μM of four duplexes in 50 mM, pH 8.5 Tris-Ac buffer, and also D1R2 in pH 4.5 buffer. The absorbance was monitored at 260 nm and normalized.

the band in lane 4 displaying the slowest electrophoretic mobility (lane 9, Figure 2c). A second band migrates exactly with the duplex in lane 4. Only a very small amount of single-stranded R2 is observed under these conditions (compare lane 6). This strongly suggests that R2 can combine with D1R2, and the resulting structure is an $R2^{+}$·D1R2 triplex. Although the duplex coexists with the triplex $R2^{+}$·D1R2, only one transition is observed in the melting profile of D1R2 under acidic condition (Figure 4). Interestingly, the T_m under acidic conditions increases by 7−8 °C as compared to the curve obtained at pH 8.5. This indicates the formation of a structure that exhibits higher stability than the heteroduplex, in accordance with triplex formation.

In contrast, the band pattern obtained in lane 10 of Figure 2c corresponds to that of the R1R2 duplex and the unpaired R2, indicating that the excess R2 oligonucleotide does not engage in triplex formation with the R1R2 duplex. A likely explanation for the difference in the tendency to form a triple helix between R2 and the two duplexes may be the lower relative stability of an RNA·RNA−RNA triplex as compared to that of an RNA·DNA−RNA triplex under identical conditions.[27,36,37] Alternatively, the deep major groove of an A-form RNA helix is more rigid than DNA/RNA heteroduplexes, which adopt a conformation between A- and B-form. The latter thus may be more accessible to a third strand than the rigid RNA−RNA duplex, although all-RNA triplexes have been described.[27,36]

The addition of K^{+} at pH 4.5 results in two major changes in PAGE (Figure 2d) when compared to Figure 2c. Similar to the observation at pH 8.5, multimers of DNA and RNA G-quadruplexes are also obtained at pH 4.5 in the presence of K^{+} (lanes 1, 3, 5, 7). However, the monomer of the R1 G-quadruplex (lane 7) is not observed; this G-quadruplex mainly exists in the dimer and trimer forms. Another significant change occurs to the $R2^{+}$·D1R2 triplex. The band that corresponds to the triplex nearly disappears (lane 4), whereas the bands of both D1 and R2 are present, indicating that the triplex unwinds in the presence of K^{+}. This is expected as K^{+} promotes the folding of D1 into G-quadruplex. The corresponding CD spectrum also confirms this transition from triplex to G-quadruplex, evidenced by the typical CD characteristics of parallel G-quadruplex rather than triplex (Figure 3d; see also Figure S5 for CD spectra of each duplex under the four conditions).

Note that the cationic carbocyanine dye, "Stains-All", can differentially stain nucleic acid components. Under the conditions employed here, the C-rich oligonucleotides (DNA and RNA) are stained in pink or purple, independent of nucleic acid folds and salt content. G-rich oligonucleotides appear in cyan in the absence of K^{+}, and turn light blue with K^{+}, independent of the pH value. Most of the duplex motifs stain in blue, except for R1D2 in purple. The $R2^{+}$·D1R2 triplex is in purple. The respective color schemes of the individual motifs provide further evidence for motif transitions, especially for structures with similar electrophoretic mobility, and are in accordance with our various structural assignments.

On the basis of these observations described above, we conclude that the four different duplexes respond differently to the addition of K^{+} and H^{+}, respectively. Both K^{+} and H^{+} can induce the DNA duplex D1D2 to convert into a G-quadruplex or an i-motif, while neither of them triggers the structural change of the RNA duplex R1R2. The hybrid duplex D1R2 also responds to both K^{+} and H^{+}; here, the triplex is formed instead of i-motif in the presence of H^{+}. The hybrid duplex R1D2 only unwinds at acidic pH. To further interpret these differences, we determined the T_m of the four duplexes by analyzing their thermal melting curves (Figure 4). Overall, the stability of the four duplexes decreases in the order: RNA > RNA/DNA hybrid > DNA, consistent with previous observations.[38,39] The stability of D1D2 and D1R2 is relatively low; as a result, they most easily undergo the structural conversion upon addition of K^{+} and H^{+}. In contrast, the RNA duplex R1R2 is so stable that it stays intact under the same conditions. R1D2 exhibits moderate stability, and so this duplex partly unwinds upon addition of K^{+} (Figure 2b). Its complete structural conversion is only observed when the stable helical structures of R1 and D2 are formed together at acidic pH (Figure 2c and d). All structural conversions in this study are summarized in Figure 5a, which helps to completely understand distinct logic behaviors of four duplexes in the presence of different peroxidase substrates (vide infra).

A Versatile Molecular Logic Device Built on Nucleic Acid Helices. The structural conversion of nucleic acid helices may find applications in some fields. As a proof-of-concept experiment, we devise multiple logic gates based on nucleic acid structural conversion, where two triggering ions (K^{+} and H^{+}) serve as the inputs (Figure 1b). The logic output of this system relies on the peroxidase activity of DNA and RNA G-quadruplexes combined with a catalytic cofactor hemin.[40,41] There are some appropriate peroxidase substrates such as scopoletin (Sc), Amplex Red (AR), and 3,3′,5,5′-tetramethylbenzidine (TMB) for different detection means (Figure 5b). In the presence of hemin, both D1 and R1 have a moderate catalytic activity toward the H_2O_2-mediated oxidation of Sc, AR, and TMB under appropriate conditions (see Figure S6 in the Supporting Information), which enables the hemin−G-quadruplex complex to serve as the reporter in this logic system.

Sc is a fluorescent substrate that can be oxidized to a nonfluorescent product of unknown structure, catalyzed by HRP (Figure 5b).[42] Here, it also proves as a substrate suitable for the HRP-mimicking hemin−G-quadruplex complex (see Figure S6a in the Supporting Information). Two additional features make this substrate interesting with respect to being used for logic-gate operations: (1) Sc is H_2O_2-resistant in the absence of catalysts; and (2) it is highly sensitive to pH; at low pH its fluorescence is remarkably reduced as compared to pH above 8. These factors would make Sc suitable for application in a NOR logic gate operation, as the two inputs K^{+} and H^{+}

dx.doi.org/10.1021/ja2108883 | J. Am. Chem. Soc. 2012, 134, 3508−3516

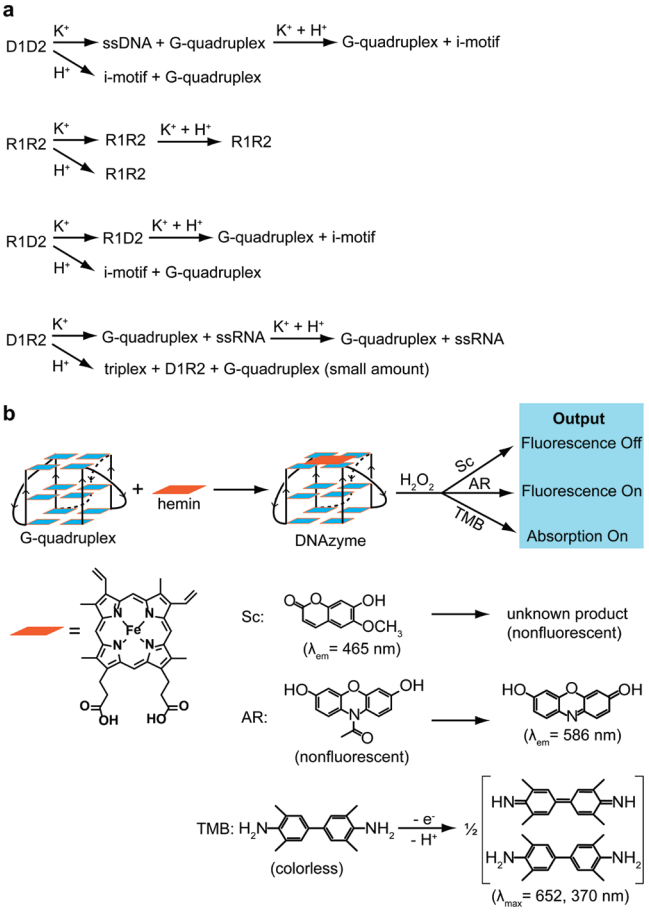

Figure 5. Summary of strand interconversions under the different conditions employed and detection of G4 formation. (a) Overview of the structural conversion of nucleic acid helices triggered by K^+ and H^+. (b) The signal output of the logic system built on nucleic acid helices. DNA or RNA G-quadruplex combines with the catalytic cofactor hemin and exhibits peroxidase activity in the presence of substrates Sc, AR, and TMB, resulting in a change in the readout signal. For TMB oxidation, only the initial blue product is shown here.

both cause a decrease in the fluorescence intensity of Sc during the structural conversion.

Figure 6 shows different logic behaviors of four duplexes at four input modes in the presence of Sc. Without any input, fluorescence intensity of Sc is high in four cases, because no hemin−G-quadruplex complex is formed. Upon input of K^+, the fluorescence decreases sharply in two cases (D1D2 and D1R2), resulting from the oxidation of Sc catalyzed by hemin−D1 complex. This means the K^+-triggered unwinding of two duplexes and the formation of G-quadruplex, consistent with the observations in PAGE and CD measurements. In contrast, the fluorescence does not decreases so obviously in the other two cases (R1R2 and R1D2), attributed to no or only partial unwinding of these duplexes as evidenced by PAGE. In the presence of H^+, the fluorescence intensity is always low due to acid quenching. With a threshold of 0.5 for logic output (1/0), both D1D2 and D1R2 behave as a two-input NOR logic gate, while R1R2 and R1D2 behave as an INV gate inverting the logic input (1/0) of H^+.[43] The corresponding truth tables of these logic gates are shown in Table 1.

AR is another peroxidase substrate for fluorometric H_2O_2 determination catalyzed by HRP,[44] and has also been applied to the hemin−G-quadruplex complex.[45] Unlike Sc, AR itself has no fluorescence behavior, but its enzymatic oxidation product (resorufin) is highly fluorescent (Figure 5b).[46] Similarly, the fluorescence of resorufin is sensitive to pH and quenched by acids.[46] These factors enable the utilization of AR as another peroxidase substrate to devise an INH logic gate based on the K^+−H^+-triggered structural conversion of four duplexes. Figure 7 shows that in the absence of K^+ and H^+, the fluorescence intensity is always low in four cases. Under this condition, the background fluorescence originates from slow catalysis by unbound hemin. Upon input of K^+, the fluorescence increases sharply in two cases (D1D2 and D1R2), attributed to the production of resorufin from AR oxidation catalyzed by hemin−G-quadruplex complex. In contrast, R1R2 and R1D2 cannot cause an obvious increase in fluorescence intensity, because they are unable to completely unwind to release the G-quadruplex. In the presence of H^+, the fluorescence intensity is always close to zero due to acid quenching. With the output threshold of 0.5, the logic behaviors of D1D2 and D1R2 are consistent with a two-input INH gate, while both R1R2 and R1D2 behave as a ZERO gate that always outputs 0.[43] The truth tables of these logic gates are shown in Table 1.

We notice that in the presence of Sc and AR, the structural conversion of nucleic acid helices occurring at acidic pH cannot be exactly reflected by fluorescence change, due to their pH-sensitive properties. In principle, this is achievable using a pH-resistant substrate instead of them. However, most fluorescent peroxidase substrates are sensitive to pH and lose their fluorescent activity under acidic conditions. Therefore, we turned to colorimetric substrates instead of fluorogenic ones to be able to signal at acidic pH. TMB is one of the proper candidates. In contrast to Sc and AR, TMB is an acid-favored

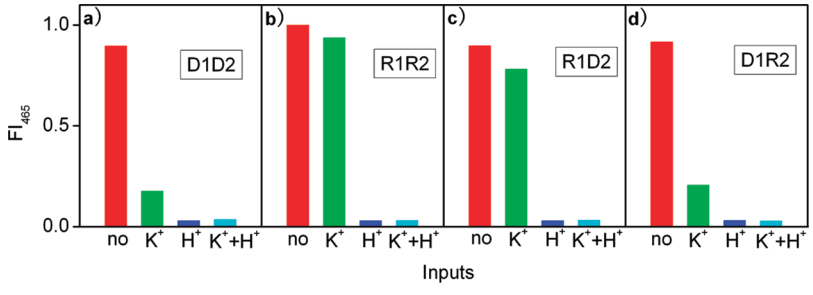

Figure 6. Logic behaviors of four duplexes in the presence of Sc at the four input modes: no input, 20 mM K^+, H^+ (pH 8.5→4.5), K^+ + H^+. Experimental conditions: 1 μM duplex + 1 μM hemin, 10 μM Sc + 50 μM H_2O_2 (9 min reaction), λ_{ex} = 390 nm. The fluorescence intensity at 465 nm (FI_{465}) was normalized, serving as the output (1/0) with a threshold of 0.5. See Supporting Information Figure S8 for the corresponding fluorescence spectra.

dx.doi.org/10.1021/ja2108883 | J. Am. Chem. Soc. 2012, 134, 3508−3516

Table 1. Truth Tables for NOR, INH, AND, and Other Logic Gates

inputs		outputs											
		O_1 (FI_{465})				O_2 (FI_{586})				O_3 (A_{652})			
I_1 (K^+)	I_2 (H^+)	D1D2 (NOR)	R1R2 (INV I_2)	R1D2 (INV I_2)	D1R2 (NOR)	D1D2 (INH)	R1R2 (ZERO)	R1D2 (ZERO)	D1R2 (INH)	D1D2 (ID I_2)	R1R2 (ZERO)	R1D2 (ID I_2)	D1R2 (AND)
0	0	1	1	1	1	0	0	0	0	0	0	0	0
1	0	0	1	1	0	1	0	0	1	0	0	0	0
0	1	0	0	0	0	0	0	0	0	1	0	1	0
1	1	0	0	0	0	0	0	0	0	1	0	1	1

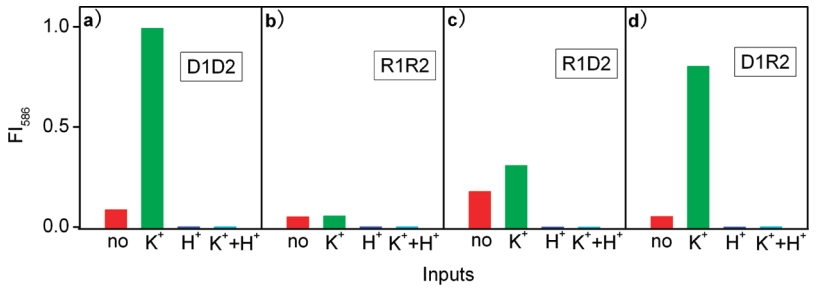

Figure 7. Logic behaviors of four duplexes with AR as the substrate at the four input modes: no input, 20 mM K^+ 3: H^+ (pH 8.5→4.5), K^+ + H^+. Experimental conditions: 1 μM duplex + 1 μM hemin, 25 μM AR + 10 μM H_2O_2 (4 min reaction), λ_{ex} = 560 nm. The fluorescence intensity at 586 nm (FI_{586}) was normalized, serving as the output (1/0) with a threshold of 0.5. See Supporting Information Figure S9 for the corresponding fluorescence spectra.

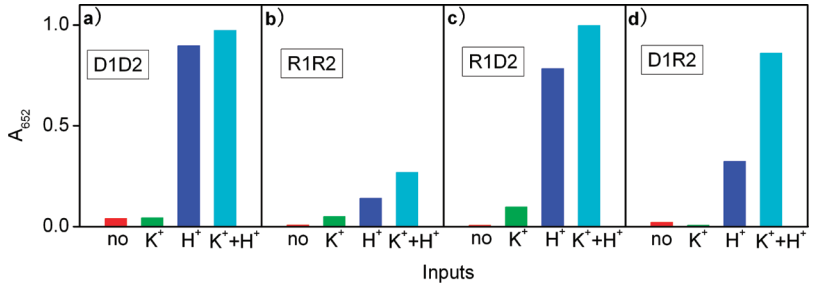

Figure 8. Logic behaviors of four duplexes with TMB as the substrate at the four input modes: no input, 20 mM K^+ 3: H^+ (pH 8.5→4.5), K^+ + H^+. Experimental conditions: 1 μM duplex + 2 μM hemin, 200 μM TMB + 1 mM H_2O_2 (60 min reaction). The maximal absorbance at 652 nm (A_{652}) was normalized, serving as the output (1/0) with a threshold of 0.5. In panel d, the H^+ signal is low (0), as in Figure 2c only a very small amount of G4 was detected with D1R2 at pH 4.5. See Supporting Information Figure S10 for the corresponding fluorescence spectra.

peroxidase substrate, which can be oxidized to colored products (Figure 5b) catalyzed by HRP[47] or the hemin–G-quadruplex complex[48] under acidic conditions. Note that the enzymatic oxidation of TMB is very slow and results in two colored products, blue and yellow, over different reaction periods.[47] Under our conditions, the time-dependent reaction shows that the initial blue product of TMB is dominant within several hours (see Figure S7 in the Supporting Information). The reaction solution then gradually turns to green, a mixture of the initial blue product and final yellow product.[47]

With TMB as the substrate, the existence of hemin–G-quadruplex complex can be detected in the presence of both H^+ and K^+, which meets the need of devising an AND logic gate (Figure 8). However, both hemin–D1 and hemin–R1 exhibit the peroxidase activity independent of K^+ (see Figure S6c in the Supporting Information), because D1 and R1 can fold into G-quadruplex even in the absence of metal cations (Figure 3c, right panel). As a result, D1D2 and R1D2 always output 1 in acidic pH and 0 in basic pH, consistent with an ID logic gate that always identifies with the logic input of H^+.[43] In the presence of H^+ alone, D1R2 forms a triplex and only releases a small amount of G-quadruplex. In this case, the catalytic activity is not so high (output 0), and thus D1R2 behaves as a two-input AND logic gate. For R1R2, it is still consistent with a ZERO gate. The truth tables of these logic gates are shown in Table 1. Note that reversible logic gates might be obtained simply by reverting the H^+- and K^+-triggered structural conversions.[49] This might provide access to more complex computing circuits.

CONCLUSIONS

We have utilized a nucleic acid system consisting of G-rich and C-rich complementary strands to study the K^+–H^+-triggered conversion of multiple helical structures involving duplexes, triplexes, G-quadruplexes, and i-motif. Four A-form and B-form duplexes are formed by hybridizing two complementary strands, evidenced by PAGE and CD. Upon addition of K^+, the DNA and DNA/RNA hybrid duplexes are subject to unwinding (albeit not completely in some cases), resulting from the formation of G-quadruplexes by G-rich strands. The multimers (dimer and trimer) of DNA and RNA G-quadruplexes were observed in PAGE, together with monomers. H^+ is also able to trigger the unwinding of DNA and DNA/RNA duplexes, attributed to the formation of an i-motif

dx.doi.org/10.1021/ja2108883 | J. Am. Chem. Soc. 2012, 134, 3508–3516

structure or a Y·RY parallel triplex. PAGE evidences at least two isomers of an intermolecular i-motif. At acidic pH, the formed triplex also undergoes a structure conversion upon addition of K^+, because the G-rich strand is prone to fold into G-quadruplex. In all cases, the RNA duplex is always kept unchanged due to high stability.

Further, the K^+−H^+-triggered structural changes of nucleic acid helices have been utilized to build a versatile molecular logic device. Here, K^+ and H^+ serve as two inputs, and the released G-quadruplex behaves as the reporter for signal output. After being bound by the cofactor hemin, DNA and RNA G-quadruplexes exhibit peroxidase activity in the presence of substrates Sc, AR, and TMB, resulting in a fluorescence or color change. Multiple logic gate operations (NOR, INH, AND, etc.) are achieved with fluorometry and colorimetry, by means of different catalytic behaviors of hemin−G-quadruplex complex in three peroxidase substrates.

Our study provides rich and useful information for the interconversion of nucleic acid helical structures, which helps to further devise molecular machines and nanodevices built on nucleic acids. For example, this trigger-switched system may also function in the context of larger DNA-nanoarchitectures and nanomachines with programmable functionalities,[50] such as interlocked dsDNA-nanostructures like DNA rotaxanes[51] or catenanes.[52] From the point of view of molecular computing, the development of versatile logic devices will facilitate constructing more advanced molecular calculators or computing circuits.

■ ASSOCIATED CONTENT

Supporting Information

Melting profiles of G-quadruplexes and i-motif, proposed structures of G4 multimers and i-motif isomers, concentration-dependent T_m of D2, CD spectral change of four duplexes, catalytic behaviors of D1 and R1, time-dependent H_2O_2-mediated oxidation of TMB, and raw spectral data for logic operations. This material is available free of charge via the Internet at http://pubs.acs.org.

■ AUTHOR INFORMATION

Corresponding Author

m.famulok@uni-bonn.de

Notes

The authors declare no competing financial interest.

■ ACKNOWLEDGMENTS

This work is supported by grants from the Alexander von Humboldt Foundation, the ERC, the ESF, and the SFB 624.

■ REFERENCES

(1) Watson, J. D.; Crick, F. H. *Nature* **1953**, *171*, 737−738.
(2) Fox, K. R. *Curr. Med. Chem.* **2000**, *7*, 17−37.
(3) Frank-Kamenetskii, M. D.; Mirkin, S. M. *Annu. Rev. Biochem.* **1995**, *64*, 65−95.
(4) Gehring, K.; Leroy, J. L.; Gueron, M. *Nature* **1993**, *363*, 561−565.
(5) Snoussi, K.; Nonin-Lecomte, S.; Leroy, J. L. *J. Mol. Biol.* **2001**, *309*, 139−153.
(6) Leroy, J. L.; Gueron, M.; Mergny, J. L.; Helene, C. *Nucleic Acids Res.* **1994**, *22*, 1600−1606.
(7) Mergny, J. L.; Lacroix, L.; Han, X. G.; Leroy, J. L.; Helene, C. *J. Am. Chem. Soc.* **1995**, *117*, 8887−8898.
(8) Sen, D.; Gilbert, W. *Nature* **1990**, *344*, 410−414.
(9) Gellert, M.; Lipsett, M. N.; Davies, D. R. *Proc. Natl. Acad. Sci. U.S.A.* **1962**, *48*, 2013−2018.
(10) Williamson, J. R. *Annu. Rev. Biophys. Biomol. Struct.* **1994**, *23*, 703−730.
(11) Sen, D.; Gilbert, W. *Biochemistry* **1992**, *31*, 65−70.
(12) Smargiasso, N.; Rosu, F.; Hsia, W.; Colson, P.; Baker, E. S.; Bowers, M. T.; De Pauw, E.; Gabelica, V. *J. Am. Chem. Soc.* **2008**, *130*, 10208−10216.
(13) Martadinata, H.; Phan, A. T. *J. Am. Chem. Soc.* **2009**, *131*, 2570−2578.
(14) Collie, G. W.; Parkinson, G. N.; Neidle, S.; Rosu, F.; De Pauw, E.; Gabelica, V. *J. Am. Chem. Soc.* **2010**, *132*, 9328−9334.
(15) Phan, A. T.; Mergny, J. L. *Nucleic Acids Res.* **2002**, *30*, 4618−4625.
(16) Risitano, A.; Fox, K. R. *Biochemistry* **2003**, *42*, 6507−6513.
(17) (a) Choi, J.; Majima, T. *Chem. Soc. Rev.* **2011**, *40*, 5893−5909. (b) Lacroix, L.; Mergny, J. L.; Leroy, J. L.; Helene, C. *Biochemistry* **1996**, *35*, 8715−8722.
(18) Kolpashchikov, D. M.; Stojanovic, M. N. *J. Am. Chem. Soc.* **2005**, *127*, 11348−11351.
(19) Elbaz, J.; Lioubashevski, O.; Wang, F.; Remacle, F.; Levine, R. D.; Willner, I. *Nat. Nanotechnol.* **2010**, *5*, 417−422.
(20) Win, M. N.; Smolke, C. D. *Science* **2008**, *322*, 456−460.
(21) Szacilowski, K. *Chem. Rev.* **2008**, *108*, 3481−3548.
(22) Travascio, P.; Li, Y.; Sen, D. *Chem. Biol.* **1998**, *5*, 505−517.
(23) Travascio, P.; Bennet, A. J.; Wang, D. Y.; Sen, D. *Chem. Biol.* **1999**, *6*, 779−787.
(24) Kypr, J.; Kejnovska, I.; Renciuk, D.; Vorlickova, M. *Nucleic Acids Res.* **2009**, *37*, 1713−1725.
(25) Salazar, M.; Fedoroff, O. Y.; Miller, J. M.; Ribeiro, N. S.; Reid, B. R. *Biochemistry* **1993**, *32*, 4207−4215.
(26) Bhattacharyya, A.; Murchie, A. I.; Lilley, D. M. *Nature* **1990**, *343*, 484−487.
(27) Roberts, R. W.; Crothers, D. M. *Science* **1992**, *258*, 1463−1466.
(28) Ratmeyer, L.; Vinayak, R.; Zhong, Y. Y.; Zon, G.; Wilson, W. D. *Biochemistry* **1994**, *33*, 5298−5304.
(29) Gulik, A.; Inoue, H.; Luzzati, V. *J. Mol. Biol.* **1970**, *53*, 221−238.
(30) Scheerhagen, M. A.; Bokma, J. T.; Vlaanderen, C. A.; Blok, J.; van Grondelle, R. *Biopolymers* **1986**, *25*, 1419−1448.
(31) Hazel, P.; Huppert, J.; Balasubramanian, S.; Neidle, S. *J. Am. Chem. Soc.* **2004**, *126*, 16405−16415.
(32) Rachwal, P. A.; Findlow, I. S.; Werner, J. M.; Brown, T.; Fox, K. R. *Nucleic Acids Res.* **2007**, *35*, 4214−4222.
(33) Bugaut, A.; Balasubramanian, S. *Biochemistry* **2008**, *47*, 689−697.
(34) Mergny, J. L.; Lacroix, L. *Oligonucleotides* **2003**, *13*, 515−537.
(35) Gueron, M.; Leroy, J. L. *Curr. Opin. Struct. Biol.* **2000**, *10*, 326−331.
(36) Han, H. Y.; Dervan, P. B. *Proc. Natl. Acad. Sci. U.S.A.* **1993**, *90*, 3806−3810.
(37) Escude, C.; Francois, J. C.; Sun, J. S.; Ott, G.; Sprinzl, M.; Garestier, T.; Helene, C. *Nucleic Acids Res.* **1993**, *21*, 5547−5553.
(38) Lesnik, E. A.; Freier, S. M. *Biochemistry* **1995**, *34*, 10807−10815.
(39) Barone, F.; Cellai, L.; Matzeu, M.; Mazzei, F.; Pedone, F. *Biophys. Chem.* **2000**, *86*, 37−47.
(40) Kong, D. M.; Yang, W.; Wu, J.; Li, C. X.; Shen, H. X. *Analyst* **2010**, *135*, 321−326.
(41) Cheng, X.; Liu, X.; Bing, T.; Cao, Z.; Shangguan, D. *Biochemistry* **2009**, *48*, 7817−7823.
(42) Miller, R. W.; Sirois, J. C.; Morita, H. *Plant Physiol.* **1975**, *55*, 35−41.
(43) Rurack, K.; Trieflinger, C.; Koval'chuck, A.; Daub, J. *Chem.-Eur. J.* **2007**, *13*, 8998−9003.
(44) Zhou, M. J.; Diwu, Z. J.; PanchukVoloshina, N.; Haugland, R. P. *Anal. Biochem.* **1997**, *253*, 162−168.
(45) Li, C. L.; Liu, K. T.; Lin, Y. W.; Chang, H. T. *Anal. Chem.* **2011**, *83*, 225−230.
(46) Towne, V.; Will, M.; Oswald, B.; Zhao, Q. J. *Anal. Biochem.* **2004**, *334*, 290−296.

(47) Josephy, P. D.; Eling, T.; Mason, R. P. *J. Biol. Chem.* **1982**, *257*, 3669−3675.
(48) Li, T.; Li, B.; Wang, E.; Dong, S. *Chem. Commun.* **2009**, 3551−3553.
(49) (a) Liu, D.; Balasubramanian, S. *Angew. Chem., Int. Ed.* **2003**, *42*, 5734−5736. (b) Sannohe, Y.; Endo, M.; Katsuda, Y.; Hidaka, K.; Sugiyama, H. *J. Am. Chem. Soc.* **2010**, *132*, 16311−16313.
(50) (a) Teller, C.; Willner, I. *Trends Biotechnol.* **2010**, *28*, 619−628. (b) Willner, I.; Allen, V. *Org. Biomol. Chem.* **2006**, *4*, 3381−3382. (c) Alberti, P.; Bourdoncle, A.; Saccà, B.; Lacroix, L.; Mergny, J. L. *Org. Biomol. Chem.* **2006**, *4*, 3383−3391.
(51) (a) Rasched, G.; Ackermann, D.; Schmidt, T. L.; Broekmann, P.; Heckel, A.; Famulok, M. *Angew. Chem., Int. Ed.* **2008**, *47*, 967−970. (b) Mayer, G.; Ackermann, D.; Kuhn, N.; Famulok, M. *Angew. Chem., Int. Ed.* **2008**, *47*, 971−973. (c) Ackermann, D.; Schmidt, T. L.; Hannam, J. S.; Purohit, C. S.; Heckel, A.; Famulok, M. *Nat. Nanotechnol.* **2010**, *5*, 436−442. (d) Ackermann, D.; Rasched, G.; Verma, S.; Schmidt, T. L.; Heckel, A.; Famulok, M. *Chem. Commun.* **2010**, *46*, 4154−4156.
(52) (a) Weizmann, Y.; Braunschweig, A. B.; Wilner, O. I.; Cheglakov, Z.; Willner, I. *Proc. Natl. Acad. Sci. U.S.A.* **2008**, *105*, 5289−5294. (b) Schmidt, T. L.; Heckel, A. *Nano Lett.* **2011**, *11*, 1739−1742.